



HAL
open science

Thermal regime variability of islands in the Lena River near Yakutsk, eastern Siberia

François Costard, Emmanuèle Gautier, Pavel Konstantinov, Frederic Bouchard, Antoine Séjourné, Laure Dupeyrat, Alexander Fedorov

► To cite this version:

François Costard, Emmanuèle Gautier, Pavel Konstantinov, Frederic Bouchard, Antoine Séjourné, et al.. Thermal regime variability of islands in the Lena River near Yakutsk, eastern Siberia. *Permafrost and Periglacial Processes*, 2022, 33 (1), pp.18-31. 10.1002/ppp.2136 . hal-03821050v1

HAL Id: hal-03821050

<https://hal.science/hal-03821050v1>

Submitted on 21 Oct 2022 (v1), last revised 26 Sep 2023 (v2)

HAL is a multi-disciplinary open access archive for the deposit and dissemination of scientific research documents, whether they are published or not. The documents may come from teaching and research institutions in France or abroad, or from public or private research centers.

L'archive ouverte pluridisciplinaire **HAL**, est destinée au dépôt et à la diffusion de documents scientifiques de niveau recherche, publiés ou non, émanant des établissements d'enseignement et de recherche français ou étrangers, des laboratoires publics ou privés.

1 Thermal regime variability of frozen islands in the Lena River floodplain near Yakutsk, eastern Siberia

2

3 F. Costard¹, E. Gautier², P. Konstantinov³, F. Bouchard¹, A. Séjourné¹, L. Dupeyrat¹, and A. Fedorov³

4 ¹ *Université Paris-Saclay, CNRS, Laboratoire GEOPS, UMR 8148, rue du Belvédère, 91405*
5 *Orsay, France.*

6 ² *UMR 8591, Laboratoire de Géographie Physique, Meudon, France*

7 ³ *Melnikov Permafrost Institute, RAS Siberian Branch, Yakutsk, Russia*

8

9 Abstract

10 Recent evidence has shown that Arctic regions have warmed about twice as much as elsewhere on
11 the planet over the last decades, and that high-latitude permafrost-periglacial processes and
12 hydrological systems are notably responsive to rising temperatures. The aim of this paper is to report
13 on permafrost thermal regime of islands located along the Lena River floodplain, upstream of the city
14 of Yakutsk (eastern Siberia). Four islands were monitored during two consecutive years (July 2009 to
15 July 2011) to characterize their frozen soil thermal regime using waterproof dataloggers and
16 continuous monitoring of permafrost in contact with ice breakup of the Lena River. For each of these
17 islands, we measured: i) river water, air and frozen soil temperatures at different depths; ii) height of
18 ice jams; iii) submersion duration and height during the flood; iv) erosion and sedimentation. The
19 results show that within a zone of thick and continuous permafrost, the Lena River floodplain is far
20 from being homogeneous: it rather shows notably heterogeneous thermal regimes, with some
21 islands composed of permafrost and others with only seasonally frozen ground. Our study highlights
22 the complexity of ecosystem responses across Arctic environments.

23

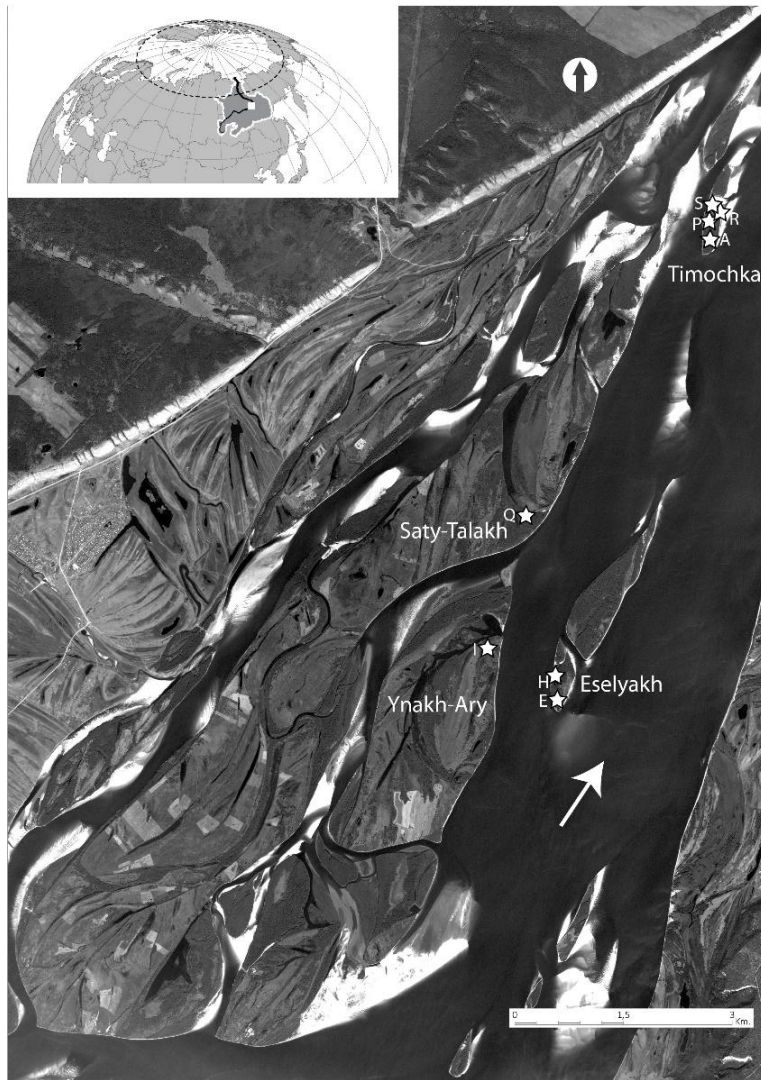
24 1. Introduction

25

26 Permafrost has been warming at the global scale over the last decade, following the Arctic
27 amplification of air temperature increase in the Northern Hemisphere (Biskaborn et al., 2019).
28 Recent work has shown a significant increase in air and ground temperatures in central Yakutia since
29 the late 1980s (Fedorov et al., 2014; Iijima et al., 2016, Zhang et al., 2012). In the lower Lena River
30 valley (Figure 1), according to Yang et al. (2002), the mean annual ground temperature has increased
31 by about 1.3°C since 1930. The mean annual air temperature at Yakutsk, which was ranging between
32 -10.3°C and -9.9° for the period 1936-1999, has increased to -7.4°C for the period 2008-2017. The
33 warming is characterized by a marked inter-seasonal evolution: a strong increase (+3°C since 2000) in
34 winter temperatures (November-March) is observed, while spring temperatures (April and May)

35 have increased by 2.3°C. The precipitation (about 230 mm per year at Yakutsk) does not show the
36 same trend, however. Very wet conditions have occurred more frequently since 1998 (1999, 2005,
37 2006, 2007 and 2013), with storms affecting Siberia resulting in more abundant late summer
38 precipitation and early winter snow (Fedorov et al., 2014b; Iijima et al., 2016).
39 Furthermore, active layer deepening results in an increase in river discharge. At the beginning of the
40 21st century, Peterson et al. (2002) reported an average increase of 7% in water discharge volumes
41 delivered by the seven main sub-arctic rivers, including the Lena. More recently, a study (Gautier et
42 al., 2018) reported a strong water discharge increase since the beginning of the 21st century for the
43 Lena River at Tabaga (just upstream of Yakutsk): the 2000-2017 discharge was 15% higher than the
44 discharge for 1936-1999. Furthermore, floods are also changing, with more frequent flood peaks and
45 longer recorded flooding durations (Gautier et al., 2018). Recent exceptional flood events are
46 reported (Shiklomanov and Lammers, 2009; Costard et al., 2014; Gautier et al., 2018; Tei et al.,
47 2020). There has also been a decrease in winter river ice cover, used as road. Winter
48 thawing/melting events, as well as spring ice jam floods during the ice breakups represent major risks
49 for riverside residents, road and river infrastructures. All these factors lead to permafrost instability
50 and consequent changes in forest, wetland, lake and river ecosystems.

51



52

53

54 Figure 1: A. Location of the Lena basin (grey-shaded area). B. Study area (upstream of Yakustk).

55 Background image: Spot 2008; Star with letters: Temperature sensors.

56

57 Very few studies have focused on geomorphological impacts of ice breakups and floods on major
 58 Arctic rivers. Most of the geomorphological studies concern river dynamics of breakup for Canadian
 59 Arctic rivers (Beltaos and Burrell, 2002). Specifically, studies have shown the role of the ice cover and
 60 its thickness on the intensity of ice jams produced by ice packs along the Yukon River (Shen, 2003;
 61 Walker and Hudson, 2003). With increasing discharge, the ice cover under pressure locally cracks and
 62 starts to move (Shen, 2003). This is the beginning of the "break up" phase where ice rafts accumulate
 63 at the head of islands (Figure 2). The flow often carries these ice blocks along with tree trunks
 64 (Walker and Hudson, 2003). Ice jams produce local dams, resulting in a sudden rise of water levels
 65 (Billfalk, 1982; Beltaos and Burrell, 2002; Costard et al., 2014). During the flooding season, a typical

66 heat exchange takes place between the water and the frozen islands, leading to accelerated erosion
67 of the banks (Are, 1983; Jahn, 1975; Walker, 1983).

68
69 Breakup is strongly heterogeneous, as numerous factors control its starting date and intensity
70 (Costard et al., 2014; Gautier et al., 2018). These events can depend on temperature and
71 precipitation within the watershed, but also on ice cover thickness, starting date and duration of the
72 break-up phase, and spring and/or winter temperatures. In Siberia, the conditions for the onset of
73 break-up events, as well as their intensity or efficiency on erosion, remain poorly characterized.
74 Moreover, analysis of climatic and hydrological data near Yakutsk showed a very clear thinning trend
75 in winter ice thickness and a significant increase in water temperature of the Lena River near Tabaga
76 (gauging station upstream section of Yakutsk, Figure 1). We have also demonstrated (Costard et al.,
77 2007) the impact of recent warming on increasing erosion rates of the islands by thermal erosion. .

78



79
80 Figure 2: Beginning of the ice breakup on the Lena River in 2010. The Eselyakh Island is submerged.
81 Flow from right to left. During the first days, drifting ice blocks on the river form thick ice
82 accumulations at the Eselyakh Island head, together with a frontal erosion of up to 40 m within a few
83 days.

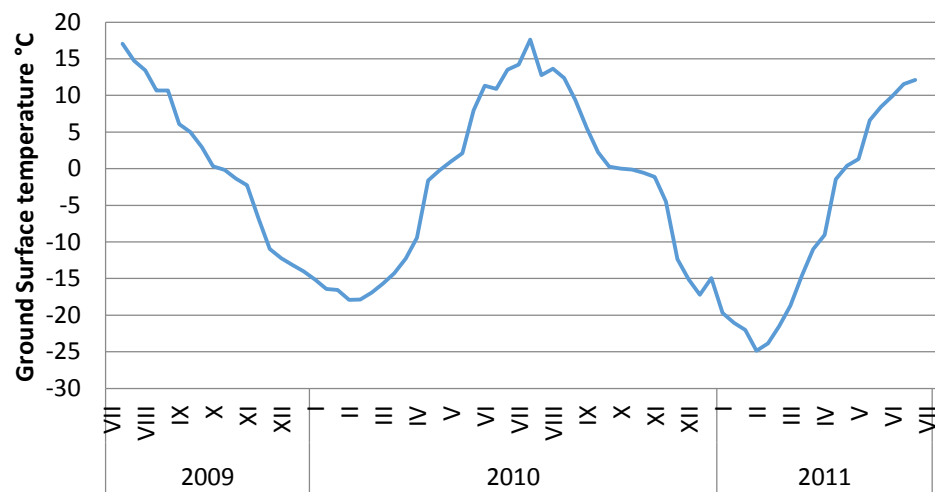
84
85 Break-up and large flooding events represent an important risk in Arctic regions and can threaten
86 infrastructures. In May 2001 and 2010, catastrophic breakup events linked to an early spring season
87 following a severe winter strongly impacted the cities of Yakutsk and Lensk (Gautier et al., 2018).
88 Recently, a project of a 6 km-long bridge across the Lena floodplain at Tabaga site is projected and it
89 implies accurate knowledge of the formation, and especially of the causes of the variable intensity of
90 these ice breakups. Specifically, there is a clear need to analyze the conditions that triggered these
91 ice breakups and their subsequent geomorphological impacts on the Lena river banks. Interestingly,
92 some key parameters remain unresolved, such as the thermal state of these frozen islands. In order

93 to document the thermal profiles of these islands and to clarify the thermal impact of these ice
 94 breakups on Lena floodplain permafrost, we started a joint research program between GEOPS and
 95 LGP laboratories near Paris and the Melnikov Permafrost Institute in Yakutsk. The main objective of
 96 this paper was to investigate the hypothesis that some of these islands contain permanently frozen
 97 soil (permafrost), while others are affected only by seasonal frost.

98

99 **2. Study area**

100 Central Yakutia (eastern Siberia) is characterized by a strongly continental climate with extreme
 101 variations in air temperatures, ranging from +40°C in summer to -60°C in winter (Fedorov et al.,
 102 2014). The region is characterized by a thick continuous ice-rich permafrost of late Pleistocene age,
 103 called “Yedoma” (Antonov, 1960; e.g., Schirrmeister et al., 2013). Figure 3 and Table 1 show the
 104 contrasted ground surface temperature range between July 2009 and July 2011, as recorded within
 105 the Lena River floodplain upstream of Yakutsk at the Eselyakh Island (for location see Figure 1). The
 106 average annual ground surface temperature is around -10°C. The low annual precipitation (230 mm
 107 near Yakutsk), together with a high evaporation rate, induces a dry climate (Antonov, 1960). The wet
 108 season occurs in the summer, with 140 mm distributed between June and September. Snow cover
 109 thickness remains low (30 to 40 cm), which favors efficient frost penetration and the existence of
 110 deep permafrost, especially underneath the taiga. Locally, permafrost has an average temperature of
 111 -5°C and a maximum depth of 1500 m (Fedorov and Konstantinov, 2009). Since the end of the 1980s,
 112 it has undergone a warming of almost 1.5°C (at a depth of 3.2 m), together with a deepening of the
 113 active layer, with values ranging from 0.8 to 1.2 m at the latitude of Yakutsk (Fedorov and
 114 Konstantinov, 2003; Fedorov et al., 2014).



115
 116
 117
 118
 119

Figure 3: Recorded ground surface temperatures of Hobo E between July 2009 and July 2011 on the Lena River floodplain at Eselyakh Island.

120 In Yakutia, the Lena River is one of the largest fluvial hydrosystems within the periglacial zone (Figure
121 1), with thick and continuous permafrost. From its large watershed (2.49 million km²), the Lena
122 annually brings 525-537 km³ of water to the Laptev Sea (Antonov, 1960; Shiklomanov et al., 2009),
123 representing 15 % of total freshwater flow into the Arctic Ocean. During the winter season, the river
124 flows under an ice cover of 1.4 m thick on average (min: 30 cm; max. 2 m). The river discharge is then
125 extremely low (less than 1500 m³ s⁻¹ at the Tabaga station, south of Yakutsk city, by 61° 4'N and 129°
126 3'E) and reaches its lowest discharge of 870 m³ s⁻¹ at the end of the cold season (Gautier and Costard,
127 2000; Gautier et al., 2018).

128
129 The four instrumented islands present various configurations. Two islands (Eselyak and Timochka)
130 are located in the central part of the active channel, whereas Ynakh-Ary and Saty-Talakh are two very
131 large lateral islands, sizing 5 km² and about 20 km², respectively (Figure 1). The islands are colonized
132 by a homogeneous alluvial forest mainly composed of willows. On the Lena River, islands are formed
133 by stabilization of sand bars by pioneer sequences. Because of the short duration of flooding in the
134 spring, sand bars are dewatered during two or three months (July-September), allowing young
135 willows to grow. Because of their abundance, young trees trap the sediment load, causing rapid
136 vertical accretion of the island (Gautier et al., 2021). Hence, the basis of the island stratigraphy is
137 mainly composed of sand, i.e. homometric ($D_{50} = 200 - 250 \mu\text{m}$) sandy material organized in
138 horizontal beds several tens of centimeters thick. The sandy deposits are often covered with layers of
139 silt (D_{50} between 50 and 100 μm) deposited by overbank flows. Thicker fine-grained deposits can be
140 found in abandoned channels. For a detailed description of the sedimentary sequences of these
141 islands, see Gautier and Costard (2000) and Costard et al. (2014).

142 On the Lena river, ice breakups are controlled by the meridian (i.e. from south to north) course of the
143 river, with a 30- to 50-day lag between basin upstream and downstream (Gautier et al., 2003). As a
144 result, a flood wave propagates from the southern regions further to the still-frozen regions in the
145 north. In spring, when snow and ice covers melt, the flow increases abruptly. Massive ice and log
146 jams can be formed on the island heads (figure 2). The ice break-up at the latitude of Yakutsk occurs
147 during the second half of May and within a few days, the volume of water flow increases by 20 to 45
148 times. The peak flood can reach up to 50,000 m³ s⁻¹ (Antonov, 1960, Liu et al., 2005; Gautier et al.,
149 2018). At the latitude of Yakutsk, that water level during the flood season can be up to 8 to 10 m
150 relative to the winter low water level (Costard et al., 2007; Gautier et al., 2018). During high floods,
151 the Lena flood spreads over a width of 25 km. The water temperature, very low in the winter and at
152 the beginning of the flooding season, increases rapidly to reach 17-18°C in July and August (Costard
153 et al., 2014).

154

155 Preliminary studies based on the analysis of satellite images had been conducted, which enabled us
 156 to identify the locations with the highest erosion rates on a 100-km long transect of the Lena River in
 157 Yakutia (Costard et al. 2007). Furthermore, more than one hundred islands have been surveyed on
 158 the basis satellite images (1967 – 2017) and erosion – sedimentation was surveyed for several years
 159 on five islands (Costard et al., 2014; Gautier et al., 2021). Thermal erosion of river banks ranges on
 160 average between 11 and 18 m yr⁻¹ on island head (upper part) and 5 to 10 m on island side. In
 161 localized areas, erosion rates of 25 to 40 m yr⁻¹ could be observed (Gautier et al., 2003; Costard et al.,
 162 2007, 2014; Tananaev, 2016; Dupeyrat et al., 2018; Gautier et al., 2021). The thermo-mechanical
 163 erosion efficiency implies that the water is permanently in contact with permafrost (Walker and
 164 Arnborg, 1963; Jahn, 1975; Walker, 1983; Costard et al., 2014).

165 For the purpose of our study, a site upstream of Yakutsk (Figure 1) have been chosen, which allows
 166 to avoid the urban heat flow. In addition, the upper Lena River is not impacted by dams. Ten islands
 167 were preselected, and four of them have been instrumented and discussed further in this paper
 168 (Figure 1). Two islands are lateral old islands and two are located in the center of the river channel.

169

170 Table 1. Main features of the 4 study islands. Letters: temperature sensors

| Island Name | Area (m ²) | | | Age | Dataloggers | | | Geomorphic Unit |
|--------------------|------------------------|------------|------------|--------|-------------------------------------|----------------------------|------------|-------------------|
| | 1967 | 2008 | 2017 | | Temp. at -3 m Mean – Max (°C) | Duration of measurement | Sediment | |
| Eselyakh | | | | | | | | |
| Upstream part | 486,726 | 198,256 | 105,520 | >60 yr | T4 | 2008 – 2011 | Mixed sed. | Abandoned channel |
| Downstream part | 416,877 | 790,189 | 675,931 | | E: -2.3/-3.1 H: -0.3/-0.6 | 2009 – 2011 2008 – 2011 | Sand | Bar |
| Timochka | | | | | | | | |
| Upstream part | 216,239 | 135,560 | 107,161 | <30 yr | A: 0.7/2.1 | 2008 – 2014 | Sand | Bar/island |
| Downstream part | 0 | 70,300 | 79,164 | | P: 0.6/1.6 | 2010 – 2014 | Sand | Bar/island |
| | | | | | R: 1.1/1.6 | 2010 – 2015 | Sand | Bar/island |
| | | | | | S: 1.1/1.6 | 2016 – 2018 | Sand | Bar/island |
| Ynakh-Ary | 5 047,718 | 5 338,126 | 5 0294,298 | >70 yr | I: -3.1/-3.4 | 2009 – 2016 | Mixed sed. | Abandoned channel |
| Saty-Talakh | 18 247,279 | 20 125,713 | 19 685,946 | >70 yr | Q: 0.3/-1.2 | 2010 – 2018 | Sand | Bar/island |

| | | | | | | | | |
|--|--|--|--|--|--|--|--|--|
| | | | | | | | | |
|--|--|--|--|--|--|--|--|--|

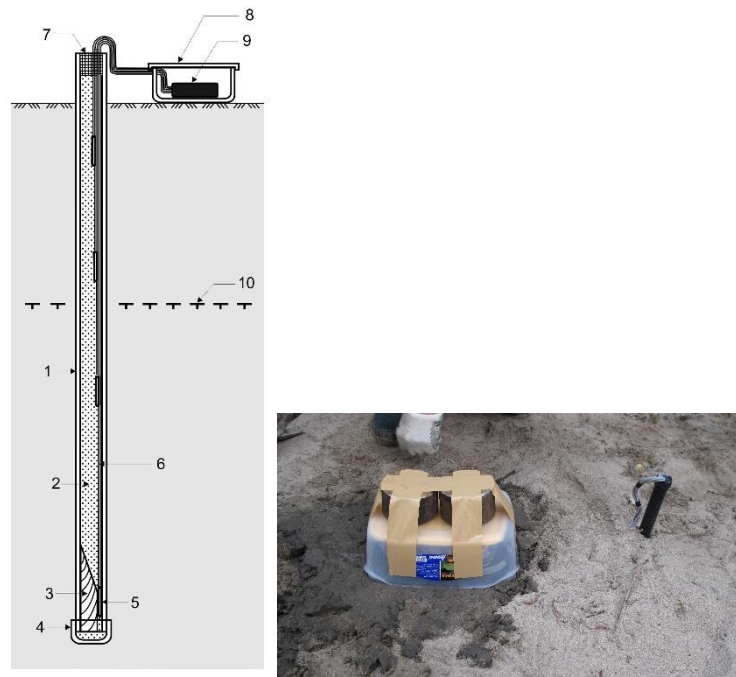
171

172 **3. Methods**

173 In order to determine the ground temperature of the islands with and without permafrost, and to
174 evaluate the active layer thickness on the islands, various methods were integrated. First, a drilling
175 campaign (2008) enabled the installation of several temperature sensors at different depths and a
176 precise measurement of the active layer. We used HOBO 4-channels dataloggers (model U12-008) to
177 record variations in the thermal profile of the frozen soil at different depths. Each datalogger,
178 previously calibrated in the laboratory, includes 4 thermocouples that automatically record, every
179 hour, permafrost and water temperature with an accuracy of $\pm 0.1^{\circ}\text{C}$, on the soil surface, at 1m, 2m
180 and 3.2 m depth (Figure 4). On Saty-Talakh island, the sensors have been installed at 2 m, 3 m and 4
181 m depth. Once a year, after the ice break-up, we went to the instrumented sites to collect data from
182 the dataloggers and to ensure the equipment maintenance on site. During the first year (2008) on
183 Timochka and Eselyakh islands, only two among the four sensors worked well and the others were
184 broken by the strong ice breakup. They were modified to ensure waterproof conditions and to
185 improve the robustness of the equipment in order to support the mechanical effect of ice breakups
186 (e.g., internal pressure). Thus, we had to develop a new system (Figure 4) that is much more efficient
187 and could support the repeated impacts of ice rafts and water pressure (Konstantinov et al., 2011).
188 Unfortunately, because of the extremely rough conditions, the duration of measurements of the
189 temperature sensors is very variable (Table 1): some of them have been working for more than 10
190 years, whereas others disappeared during a flood or were buried under meters of sediment and
191 woody debris.

192

193



194
 195 Figure 4: Photo on the left: Drilling in permafrost for the installation of thermocouples placed at 0 m,
 196 1 m, 2 m and 3.2 m depth. 1- polypropylene tube; 2- dry sand; 3-wooden bloc; 4- tube plug; 5-sensor;
 197 6-cable; 7- waterproofing compound; 8-protective box; 9-data logger; 10-bottom of active layer.
 198 Photo on the right: HOBOT datalogger modified to support flooding of the island during spring
 199 breakup. Note the 2 weights on the box and the wooden support holding the datalogger in the
 200 waterproof box. (Figure modified from Konstantinov et al., 2011).

201
 202 Other Progres-Plus Thermo-Buttons iBTag (model 22L with a $\pm 0.5^{\circ}\text{C}$ accuracy) sensors were installed
 203 on *Salix* trunks of two instrumented islands (Timoshka and Eselyakh islands) to estimate the height
 204 and duration of submersion and variations of water temperature (Costard et al., 2014; Gautier et al.,
 205 2018). These thermobuttons were installed from the ground surface and every 50 cm up to a height
 206 of 3 m. The water levels are correlated to the daily discharge measured by the navigation services at
 207 Tabaga (gauging station at 8 km from the sites). Every sensor position was precisely determined with
 208 a GPS and a total station.

209 We estimated the age of the islands based on the year of their appearance (Gautier et al., 2021) from
 210 a diachronic analysis of satellite images (Figure 10). We also used the dendrochronology method to
 211 precisely measure the age of the oldest trees. Our objectives were to identify a possible difference in
 212 their thermal regime between perennially-frozen islands and islands without permafrost (only frozen
 213 in winter).

214 We also quantified the variability of erosion and sedimentation rates over a year using field surveys
 215 (total station topographic measurements and sediment traps) and we realized various grain-size

216 analyses of the deposits (Costard et al., 2014). Here, we focus our study on the thermal regime of
217 four islands (Figure 1).

218

219 4. Results

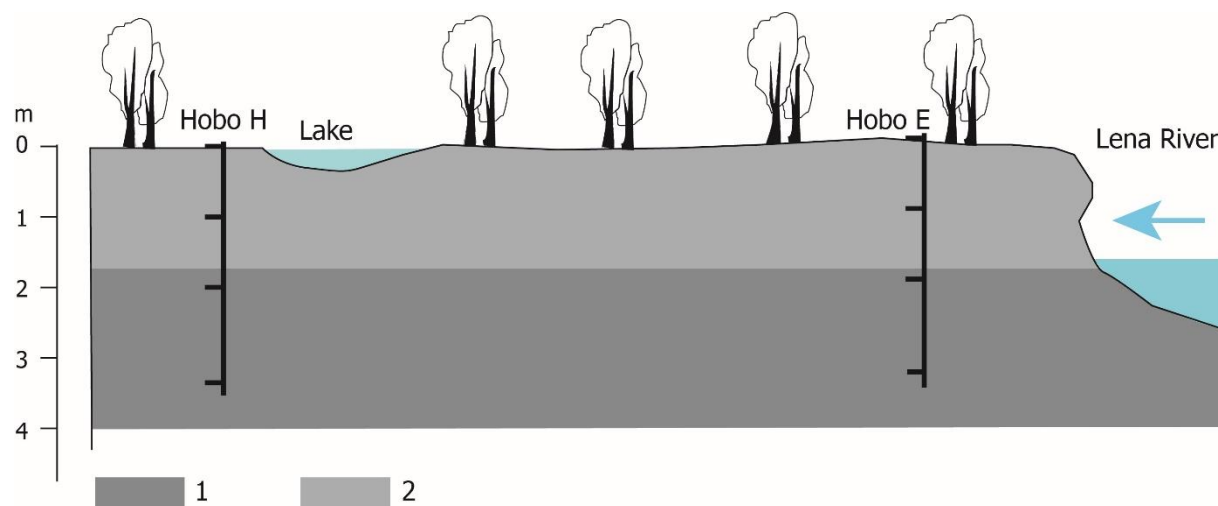
220 4.1. Islands with permafrost

221 *Thermal subsoil profiles on Eselyakh Island*

222 Based on datalogger data, we present the thermal profiles of the four islands over two consecutive
223 years between July 2009 and July 2011. The upper part of Eselyakh Island (Hobo E & H, Figures 6 and
224 7) has a permafrost with an annual average temperature of -1.3°C at 3.2 m depth. Hobo
225 measurements from successive field campaigns have shown that this permafrost is thicker on the
226 upstream section of the island (Figure 5). The soil is composed of silty-clay material.

227

228



229

230

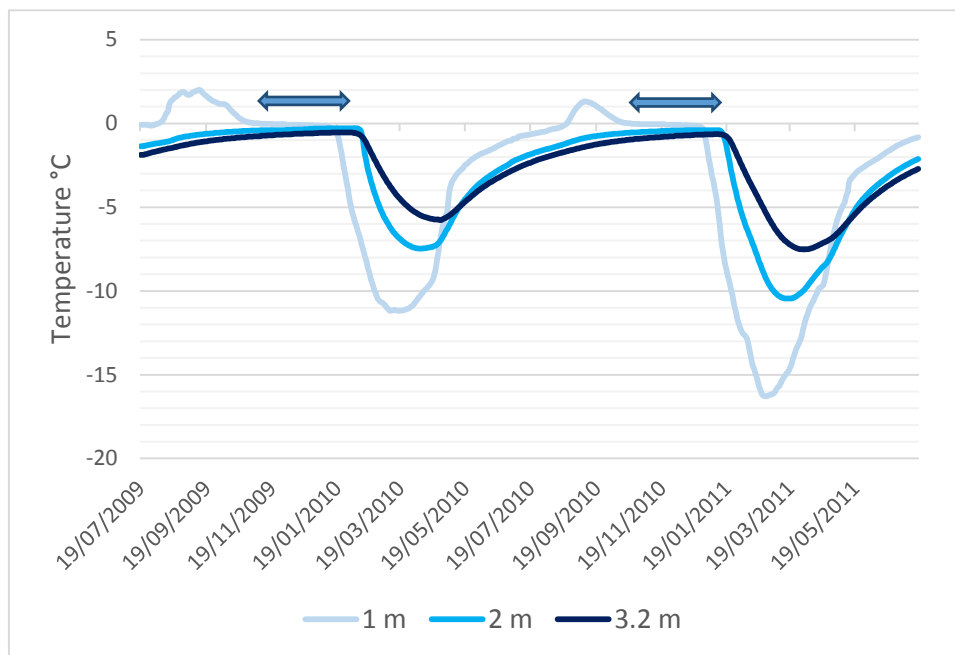
231 Figure 5: Schematic longitudinal section of Eselyakh Island. 1: permafrost; 2: active layer. Blue arrow
232 indicates flow direction (to the North). Hobo H is located near a 30 m-diameter thermokarst lake.

233

234 For this island, according to the thermal profile of HOBO E (Figure 6), permafrost temperatures
235 ranged from -0.1°C to -16.1°C at a depth of 1 m and from -0.3°C to -10.4°C at a depth of 2 m during
236 the two consecutive winters (2009 – 2010 and 2010 – 2011). At 3.2m depth, the variability of
237 permafrost temperature was even less pronounced, ranging between -0.5°C and -7.5°C . The second
238 winter was harsher: the surface temperature dropped to -25°C , and ground temperatures at 1 m, 2
239 m and 3.2 m deep reached their lowest values during this winter. The active layer is 1.6 m thick. We
240 note a downward propagation of the winter freezing wave and a time lag with depth for reaching
241 minimum temperature due to the thermal inertia of frozen ground (Figure 6). For example, the

242 minimum annual temperature was reached in early March at a depth of 1 m, in late March at 2 m,
 243 and in mid-April at 3.2 m during the first winter. This ~ 20-day time lag between different depths was
 244 also observed during the second winter, although nearly three weeks earlier than the previous year
 245 (in mid-February, early March and late March, respectively). For the October – December period,
 246 temperatures were stabilized for several weeks (from 70 to 80 days) at 0°C at a depth of 1 m at the
 247 time of freezing due to the effect of latent heat (zero curtain effect on Figure 6). At 2m- and 3.2m-
 248 depth, temperature began to decrease at the end of January. The lowest temperatures were
 249 registered in April 2010 and in March and April 2011. The permafrost here is composed of ice-rich
 250 silty clay materials (ice content around 40% by volume)

251

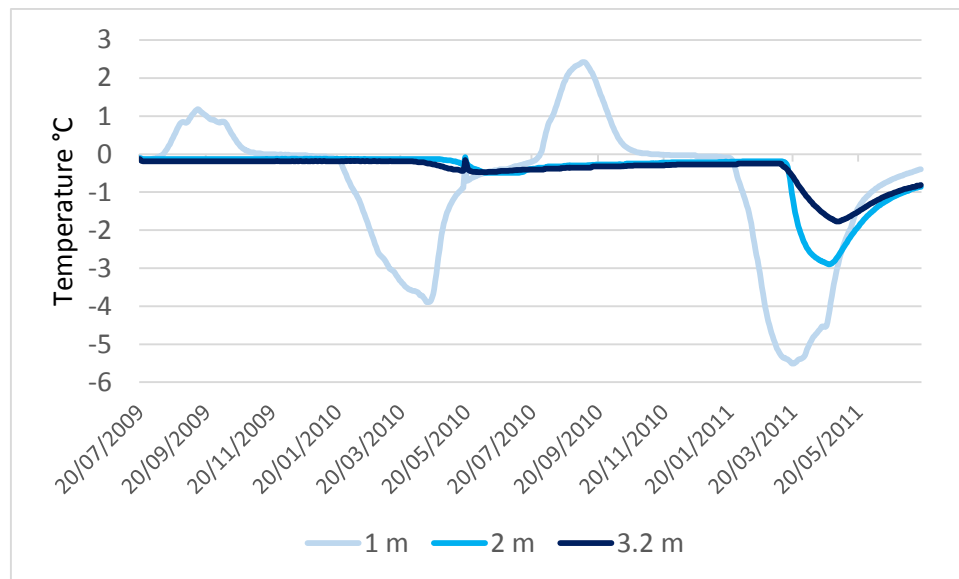


252

253

254 Figure 6: Ground thermal profiles on Eselyakh Island at 1 m, 2 m and 3.2 m depth for HOB0 E
 255 datalogger (July 2009 – July 2011). Blue arrows correspond to the zero curtain effect during phase
 256 change of the water-ice flow during breakup.

257

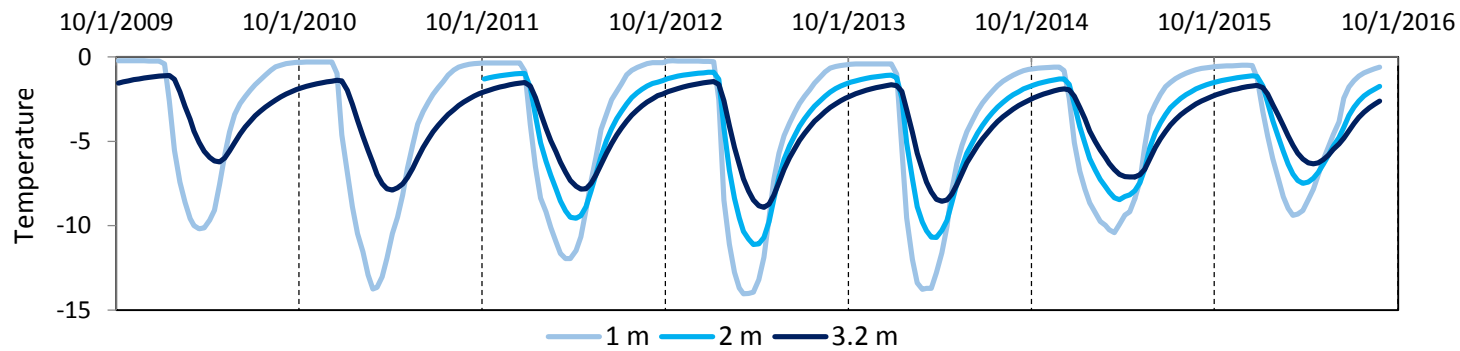


258
 259 Figure 7: Ground thermal profiles on Eselyakh Island at 1 m, 2 m and 3.2 m depth for HOBO H
 260 datalogger. (July 2009 – July 2011).

261
 262
 263 Contrastingly, the thermal profile of HOBO H, located further downstream on the island (Figure 7),
 264 shows the presence of a notably warmer permafrost. The temperature ranged between $\sim 0^{\circ}\text{C}$ and -
 265 5.5°C (1m), between -0.1°C and -2.8°C (2m) and between -0.2°C and -1.7°C (3.2m) during the second
 266 (colder) winter. Contrastingly, temperature reached -4°C at 1m and stayed around 0°C at 2 and 3.2m
 267 deep during the first (warmer) winter. In fact, this recorder is located not far from a 30 m-diameter
 268 thermokarst lake (Figure 5) corresponding to an abandoned channel, and indicates an average
 269 annual ground temperature of -0.5°C . The temperature did not vary a lot during the first winter and
 270 decreased a bit more during the second winter. The lowest temperature was registered at the end of
 271 the cold season (April, beginning of May), just before the breakup. The sediment is identical, with the
 272 same composition and grain size characteristics as on the previous site. The lake obviously induces a
 273 thermal effect by heating the upper part of permafrost, and its presence alone can explain the
 274 observed difference in the thermal regime between HOBO E and HOBO H.

275
 276 *Thermal subsoil profiles on large lateral islands (Ynakh-Ary and Saty-Talakh)*
 277 On Ynakh-Ary, Hobo I has been working from 2009 to 2016 (Figure 8). The temperature varied
 278 between -0.1 and -14°C (1m) -1.2°C and -11.1°C (2m) and between -1.2°C and -8.9°C (3.2m depth).
 279 The same progressive temperature decrease is observed, with a 2 month-time-lag separating the
 280 beginning of continuous negative temperature on the soil surface (October) and the start of the
 281 cooling within the permafrost: beginning of January at 1 m and 2 m depths, end of January or early
 282 February at 3.2m depth.

283
284



285
286

287 Figure 8: Ground thermal profiles on Ynakh-Ary island, at 1 m, 2 m and 3.2 m depth for Hobo I
288 datalogger. (October 2009 – October 2016).

289

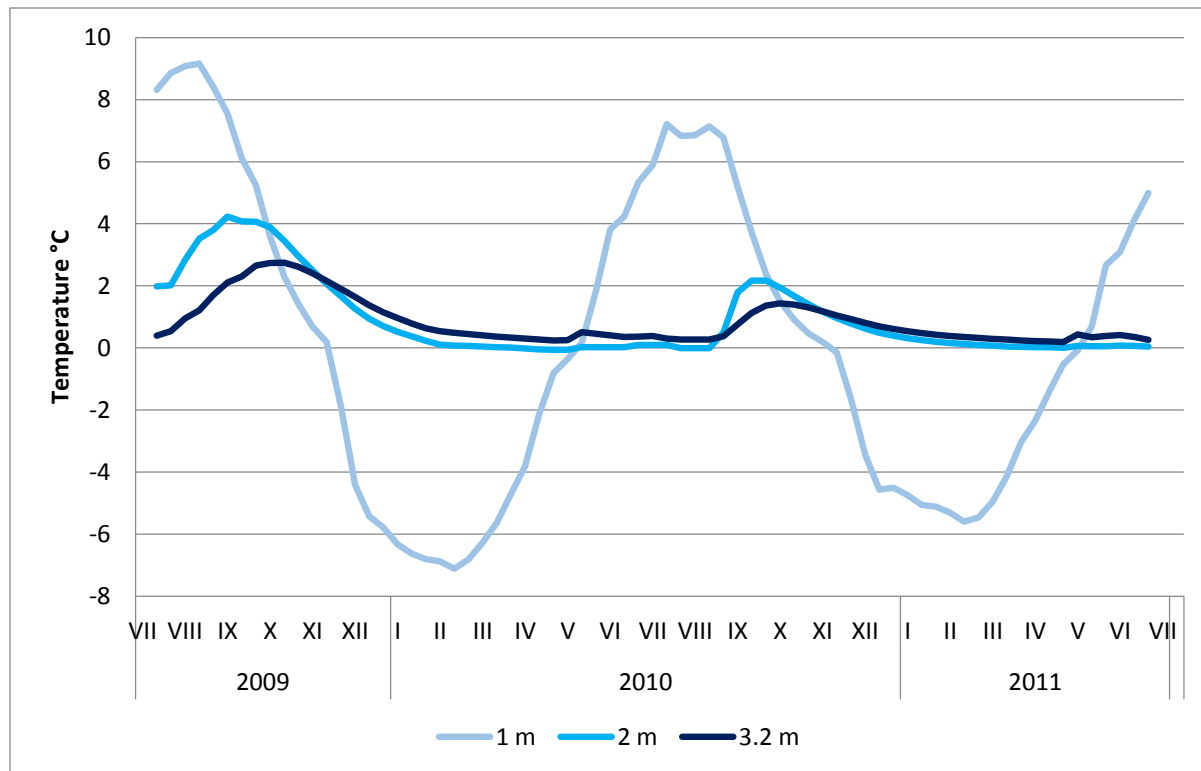
290 4.2. Islands with seasonally frozen ground

291 *Thermal subsoil profiles on Timochka Island*

292 The second instrumented island "Timochka" has a seasonal frozen ground, because the average
293 annual temperature varies between +1°C and +1.5°C at 3.2 m depth. Temperatures even remain
294 constantly above 0°C at a depth of 2 m (Figure 9). This island is mostly composed of fine sand, and
295 the willows are relatively younger than those on Eselyakh Island (from dendrochronology
296 measurements; Gautier et al., 2021).

297 These results confirm that islands like Timochka, with mainly sandy material (20% ice content by
298 volume) are less prone to the inception and development of ice-rich permafrost, whereas islands like
299 Eselyakh, containing ice-rich clay materials, are much more likely to contain ice-rich permafrost in the
300 form of segregated ice, with a much higher ice content (40% ice content by volume).

301
302
303



304
 305 Figure 9: Ground thermal profiles on Timochka Island at 1 m, 2 m and 3.2 m depths for HOB0-A, with
 306 no permafrost.

307
 308

309 **Discussion**

310

311 *Age of the islands and permafrost*

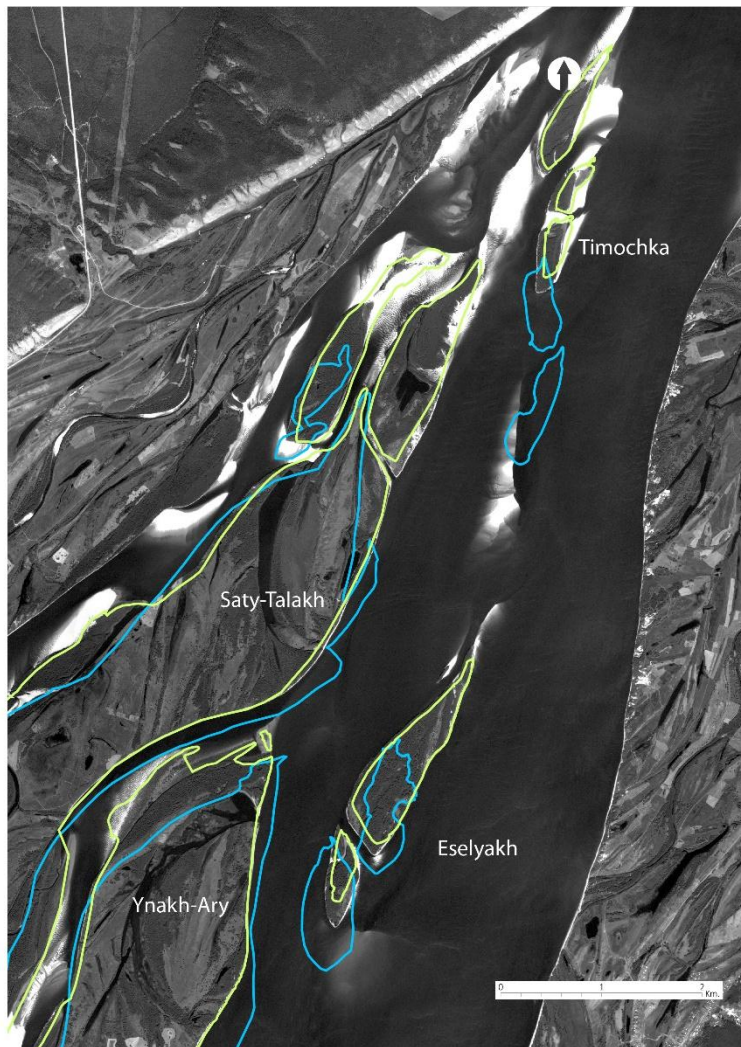
312 The middle Lena River develops a multiple-channel pattern with large forested islands (Costard et al.,
 313 2000; Gautier et al. 2008). The anabranching fluvial pattern implies relative stability of the channels
 314 and islands, although some islands quickly migrate downstream. This is the case for two islands
 315 (Eselyakh and Timochka) that are located in the central part of the active channel (Figure 1). Thus,
 316 they rapidly migrate downstream, as the head is progressively eroded, whereas the tail
 317 (downstream) progresses by deposition (Figure 10). The two other islands (Ynakh-Ary and Saty-
 318 Talakh) are large lateral islands, and are more stable.

319 Eselyakh and Timochka are bisected islands with a secondary channel between the two parts (Figure
 320 1, Table 1). Eselyakh is older than Timochka, as its two parts were already formed in 1967 (Corona
 321 pictures) and a dendrochronological analysis allows to precisely determine the age of an old willow
 322 (56 years old in 2010). This is due to the stabilization of a sand bar during the 1950's. The upper part
 323 of Eselyakh is progressively shrinking due to head erosion, whereas the lower part is growing by
 324 sedimentation. Timochka is an elongated island that is migrating very rapidly since its formation.

325 Hence, the present-day island is young: the upper part corresponds to a deposition zone formed
326 between 1980 and 1996.

327 Ynakh-Ary and Saty-Talakh are large islands with surface area of 5 km² and 20 km², respectively.
328 According to local inhabitants, they are very old islands. They were formed by the merging of
329 different islands, and lake and swamps occupy the former inter-island channels. From our study, it
330 appears that the oldest islands are thus at least 50 years old in our selected study area (Gautier et al.,
331 2021). The Ynakh-Ary, Saty-Talakh and Eselyakh islands are old islands with permafrost developed in
332 fine-grained material (silt-clay) accumulated in lower energy sections of the river, whereas Timoshka
333 Island is relatively young, with only seasonally frozen ground and mostly sand deposits accumulated
334 near the main channel, with high energy.

335



336
337 Figure 10: Main island migration on the Lena river (upstream of Yakutsk city) from GIS study. Blue line:
338 island shape in 1967 (Corona photographs); Green line: island shape 2017 (Pleiade images).

339

340 *Thermal effect of spring breakup: the example of the 2010 breakup*

341 During spring floods, the islands along the Lena River channel are submerged and this induces an
 342 additional thermal imprint. Our dataloggers were able to record this specific stage on Eselyakh and
 343 Ynakh-Ary islands (Figure 11). It can be see that the temperature variations on the ground are
 344 suddenly interrupted on May 19, 2010 with a temperature dropping and remaining at 0°C until May
 345 25, 2010 (Figure 11). This is due to the inundation of the islands where the flooding begins when the
 346 water discharge exceeds 30,000 m³.s⁻¹. The submersion duration greatly varied during the study
 347 period (Table 2).

348 Furthermore, the sensor installed at the soil surface (0 m on Figure 11) registered the water
 349 temperature. At the beginning of the flooding, temperatures close to 0°C confirm the existence of a
 350 mixture of water and ice during the break-up. Then, after a few days, the water temperature slightly
 351 increases (1°C to 3°C) as the islands are inundated by water only.

352

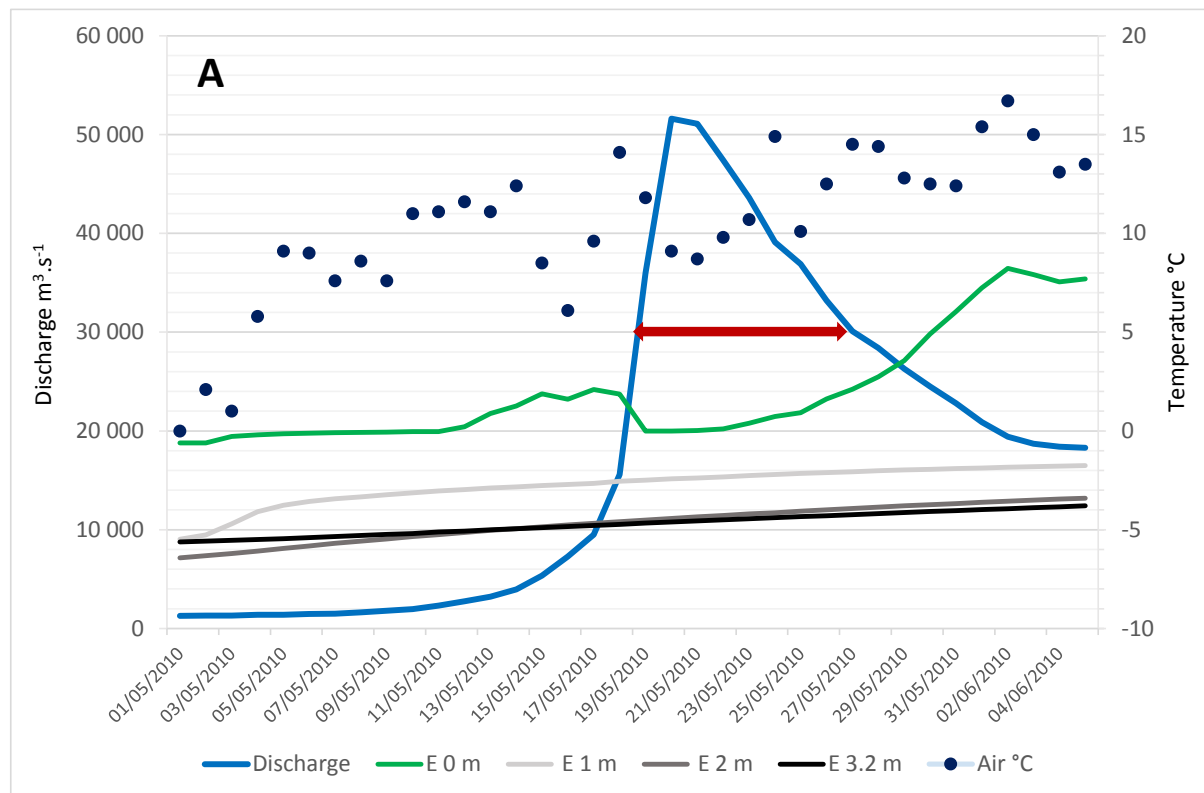
353 Table 2. Flooding characteristics

| | Flooding duration (Days) | Number flood peaks | Mean water temperature |
|------|--------------------------|--|---|
| 2009 | 26 | June 3 rd – June 28 th | ND |
| 2010 | 9 | May 19 th – May 27 th | 0°C – 0.9°C |
| 2011 | 6 | May 13 th – May 18 th | 0.2°C – 1.4°C |
| 2012 | 36 | May 17 th – May 26 th June 5 th – June 19 th July 5 th – July 9 th July 28 th – August 4 th | 0°C – 3°C 9.5°C – 12°C 15°C – 15.5°C 15°C – 16.5°C |
| 2013 | 14 | May 14 th – May 21 st July 23 rd – July 29 th | |
| 2014 | 0 | | |
| 2015 | 7 | May 13 th – May 19 th | 0.3°C – 3°C |
| 2016 | 10 | June 10 th – June 16 th July 31 st – August 3 rd | 11.6°C – 13.3°C 14.6° – 15°C |
| 2017 | 5 | July 20 th – July 24 th | ND |
| 2018 | 11 | May 5 th – May 10 th July 19 th – July 25 th | ND |

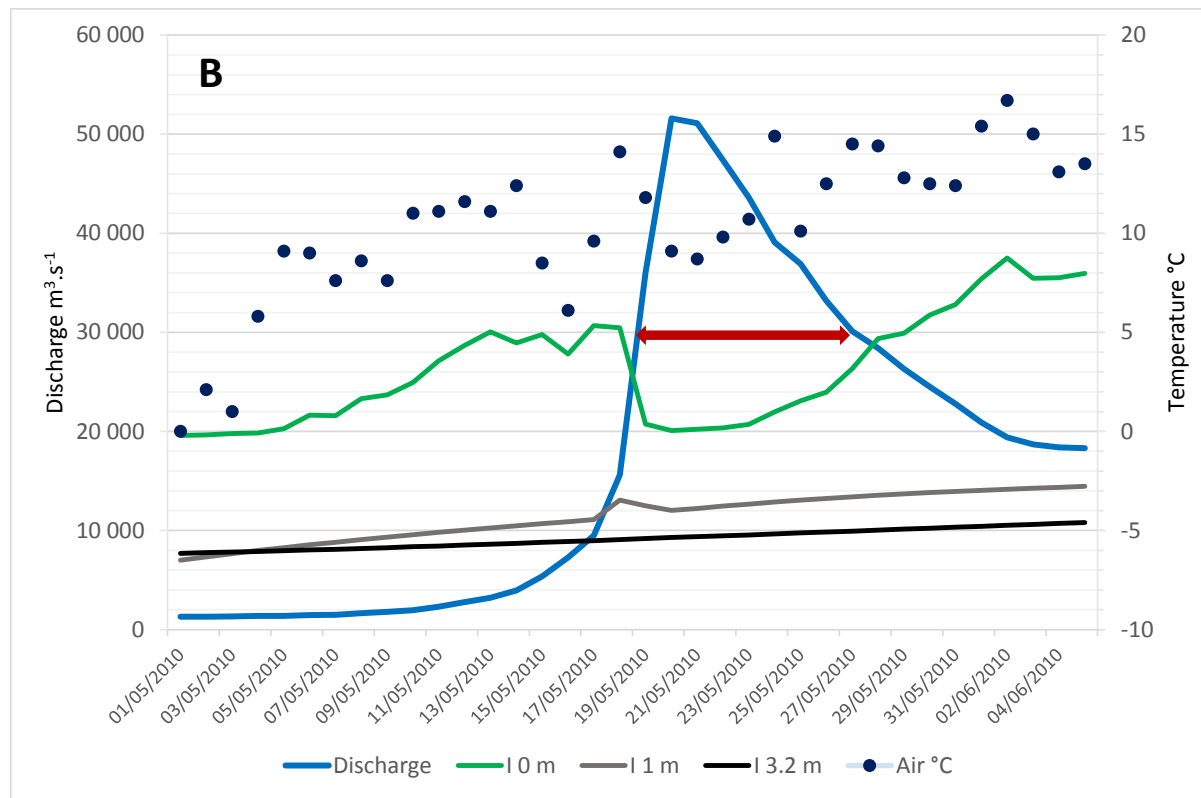
354

355

356 However, the observed effect of island submersion at the time of break-up appears to have a
 357 relatively moderated impact on permafrost thermal profile at depth (i.e. more than 1 m deep). This
 358 can likely be explained by 1) the duration of submersion, which in that case is too short to have a
 359 long-term thermal impact in the ground, and 2) the water temperature, still near 0°C, again
 360 precluding major thermal disturbance within the ground, at least below the surface. Figure 11 clearly
 361 shows that the thermal regime of permafrost for the two islands with permafrost (Eselyakh and
 362 Ynakh-Ary) did not fluctuate, even during the 10-day submersion of the island during the ice breakup
 363 in May.
 364



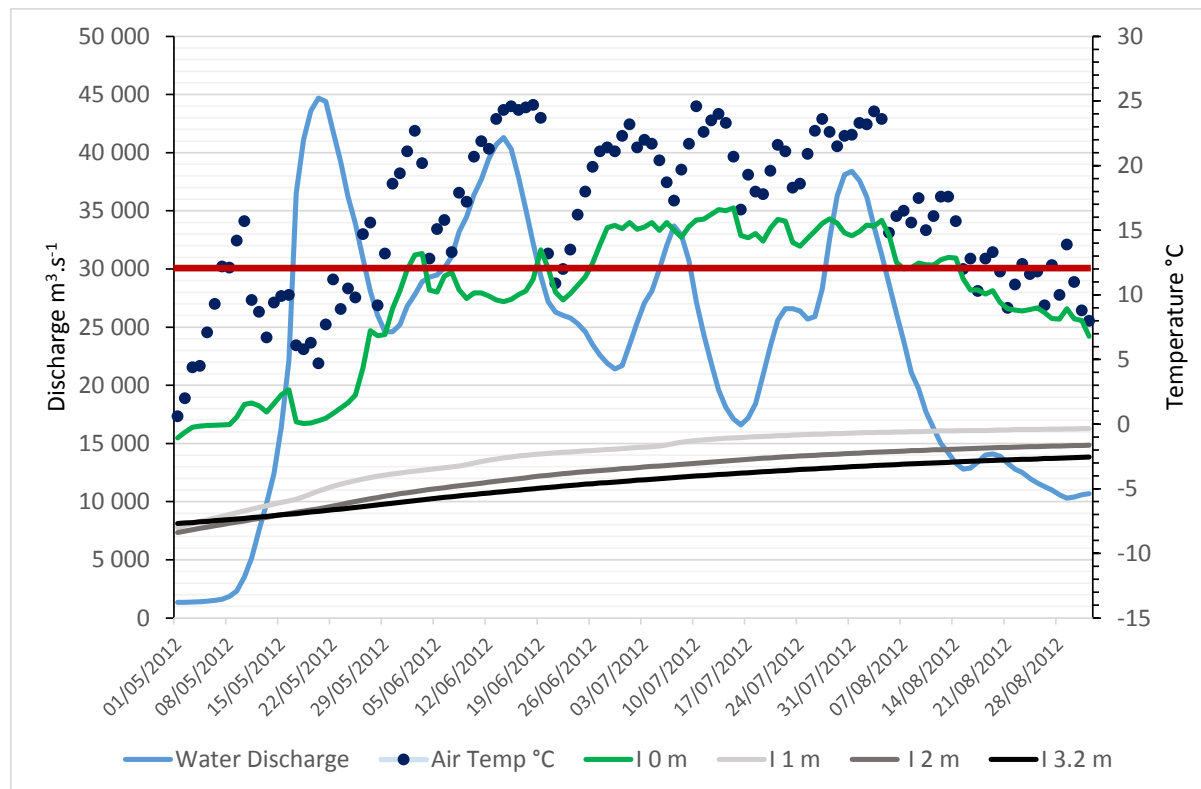
365
 366



367
 368 Figure 11: Water discharge and temperature on islands with permafrost (2010, May 1 – June 5). A:
 369 Eselyakh Island (HOB0 E), B: Ynakh-Ary Island (Sensor I). Water Discharge at Tabaga gauging station
 370 (Roshydromet data); 0 m: soil surface temperature; permafrost temperature at different depths (1
 371 m, 2 m and 3.2 m); air temperature at Yakustk (NOAA, NASA data). The red arrow corresponds to the
 372 duration of the submersion of the islands in relation with a discharge $> 30,000 \text{ m}^3 \cdot \text{s}^{-1}$.

373
 374
 375 During some years, the islands can be inundated two times or more. For example, in 2012, the Lena
 376 River underwent four flood peaks (Figure 12). This offers the possibility to examine the effect of
 377 repeated inundations and warm stream water. Even if the water temperature strongly increased
 378 from May to August, reaching $15^\circ\text{C} - 16^\circ\text{C}$ at the end of the summer, the submersion does not seem
 379 to have caused a marked increase in permafrost temperature (Figure 12).

380



381
 382 Figure 12: Water discharge, air temperature and permafrost temperature of Ynakh-Ary (HOBO I)
 383 between May and August 2012. Water Discharge at Tabaga gauging station (Roshydromet data); 0 m:
 384 soil surface temperature; permafrost temperature at different depths (1 m, 2 m and 3.2 m); air
 385 temperature at Yakutsk (NOAA, NASA data). Red horizontal line corresponds to a discharge > 30,000
 386 $\text{m}^3 \cdot \text{s}^{-1}$ in relation with the submersion of the island.

387
 388

389 Conclusions

390 For a first time, we were able to instrument a large Arctic river in order to acquire new data on the
 391 thermal impacts of ice break-up (intensity, duration, ice thickness) and flooding (water temperature,
 392 duration of submersion) on ground thermal regime. Our measurement campaigns revealed that the
 393 floodplain of the Lena River, upstream of Yakutsk, did not always contain permafrost, and that some
 394 highly mobile islands have (only) seasonally frozen ground. The Lena floodplain is notably
 395 heterogeneous, with a combination of permanently and seasonally frozen islands. The observed
 396 disparity between these instrumented islands is significant and unexpected, because it confirms that
 397 the Lena River floodplain is far from being thermally and geomorphologically homogenous. It rather
 398 consists of a juxtaposition of seasonally frozen islands and permanently frozen islands in the regional
 399 context of a floodplain affected by thick and continuous permafrost. Further surveys of 10 more
 400 islands confirm that relatively young (less than 30 years old) islands, composed of fine sand material

401 accumulated in higher energy sectors, appear less prone to permafrost formation compared to older
402 islands with ice-rich silty material deposited in lower energy environment.

403

404

405 **Acknowledgements**

406 This program was funded by ANR programs 'CLIMAFLU' (CLIMAtic change and FLUvial dynamic of the
407 Lena River, Siberia) and 'MOPGA' (Make Our Planet Great Again; through 'Projet d'Investissements
408 d'Avenir'), coordinated at GEOPS (Géosciences Paris-Saclay), Université Paris-Saclay. It also includes
409 collaborations with LGP (Laboratoire de Géographie Physique, Meudon) in France and the Melnikov
410 Permafrost Institute (Yakutsk) in Russia. All data from our field studies are presented in the
411 supplementary material S1 to S4.

412

413

414 **References :**

415 Antonov, S., 1960. Delta reki Leny. Trudy Okeanographitcheskiy Comissyi. Ak. Nauk. SSSR, 6: 25-34.

416

417 Are, F.E. (1983), Thermal abrasion on coasts, Proceedings, Fourth International Conference on
418 Permafrost, Fairbanks, Alaska, National Academy Press, Washington DC, 24-28.

419

420 Beltaos, S. and B. C. Burrell (2002), Suspended sediments concentrations during the spring breakup
421 of river ice.. In Ice in Surface Waters, Proceedings of the 14th IAHR Ice Symposium, 27-31 July 1998,
422 Postdam, N.Y. Edited by H.T. Shen. A.A. Balkema, Rotterdam, 2, 793-800.

423

424 Billfalk, L. (1982), Breakup of solid ice covers due to rapid water level variations. CRREL Report 82-3,
425 US Army CRREL, Hanover, N.H.

426

427 Biskaborn et al. 2019. Permafrost is warming at a global scale. Nature Communications, 10, 264. doi:
428 s41467-018-08240-4.

429

430 Costard F., E. Gautier, D. Brunstein, J. Hammadi, A. Fedorov, D. Yang, L. Dupeyrat (2007). Impact of
431 the global warming on the fluvial thermal erosion over the Lena river in Central Siberia. Geophys.
432 Res. Lett., 34, (14), doi:10.1029/2007GL030212

433

434 Costard F. and Gautier E. (2007). The Lena River: main hydromorphodynamic features in a deep
435 permafrost zone. In *Large rivers: Geomorphology and Management*, Gupta A (ed.). John Wiley &
436 Sons; 225-232.

437 Costard F., E. Gautier, A. Fedorov, P. Konstantinov and L. Dupeyrat. (2014). An assessment of the
438 erosional potential of fluvial thermal process during ice breakups of the Lena River (Siberia).
439 *Permafrost and Periglacial Processes*, Vol. 25, 162-171, doi:10.1002/ppp.1812
440

441 Dupeyrat, L., Hurault, B., Costard, F., Marmo, C., Gautier, E., (2018). Satellite image analysis and
442 frozen cylinder experiments on thermal erosion of periglacial fluvial islands. *Permafr. Periglac.*
443 *Process*. doi:10.1002/ppp.1973
444

445 Fedorov, A. and P. Konstantinov (2003), Observations of surface dynamics with thermokarst
446 initiation, Yukechi site, Central Yakutia. *Proceedings of International Permafrost Conference, Zurich*,
447 In *Permafrost*, Philips M., Springman S. Arenson L.U. (eds), 239-243.
448

449 Fedorov, A.N., Ivanova, R.N., Park, H., Hiyama, T., Iijima, Y., 2014. Recent air temperature changes in
450 the permafrost landscapes of northeastern Eurasia. *Polar Sci.* 8, 114–128.
451 doi:10.1016/j.polar.2014.02.001
452

453 Gautier, E. and F. Costard (2000), Les systèmes fluviaux à chenaux anastomosés en milieu
454 périglaciaire: la Léna et ses principaux affluents en Sibérie Centrale. *Géographie Physique et*
455 *Quaternaire*, 54/3, 327-342.
456

457 Gautier, E., D. Brunstein, F. Costard and R. Lodina (2003), Fluvial dynamics in a deep permafrost zone:
458 the case of the middle Lena river (Central Yakutia). *Proceedings of International Permafrost*
459 *Conference, Zurich*, Philips M., Springman S. Arenson L.U. (eds), 271-275.
460

461 Gautier E., A. Fedorov, F. Costard and D. Brunstein (2011). Impact of climate change on the dynamics
462 of a large Russian Arctic river, the Lena in Central Siberia. In *Le changement climatique. Fourth Evian*
463 *European Dialogues*. EURCASIA Ed. pp. 65-73.
464

465 Gautier, Emmanuèle, Dépret, T., Costard, F., Virmoux, C., Fedorov, A., Grancher, D., Konstantinov, P.,
466 Brunstein, D. (2018). Going with the flow: Hydrologic response of middle Lena River (Siberia) to the
467 climate variability and change. *J. Hydrol.* 557, 475–488. doi:10.1016/j.jhydrol.2017.12.034
468

469 Gautier E., Depret Th., Cavero J., Costard F., Virmoux C., Fedorov A., Konstantinov P., Jammet M., and
470 D. Brunstein (2021). Fifty-year dynamics of the Lena river islands (Russia): spatio-temporal pattern of
471 large periglacial anabranching river and influence of climate change. *Science of the Total*
472 *Environment*. In review.

473

474 Iijima, Y., Nakamura, T., Park, H., Tachibana, Y., Fedorov, A.N., 2016. Enhancement of Arctic storm
475 activity in relation to permafrost degradation in eastern Siberia. *Int. J. Climatol.* 2007.
476 doi:10.1002/joc.4629

477

478 Jahn, A. (1975), *Problems of the periglacial zone*, Washington D.C., Warszawa, 223 p.

479

480 Konstantinov, P.Y. , A.N. Fedorov, T. ?achimura, G. Iwahana, H. Yabuki, Y. Iijima, F. Costard (2011).
481 Use of automated recorders (data loggers) in permafrost temperature monitoring. *Kriosphera Zemli*,
482 1, 23-32, in russia.

483

484 Liu B., D. Yang, B. Ye, and S. Berezovskaya (2005), Long-term open-water season stream temperature
485 variations and changes over Lena River Basin in Siberia. *Global and Planetary Change*, 48, 1-3, 96-111.
486

487 Peterson, B.J., R. M. Holmes, J. W. McClelland, C. J. Vörösmarty, R. B. Lammers, A.I. Shiklomanov, I. A.
488 Shiklomanov, and S. Rahmstorf, (2002), Increasing River discharge to the Arctic Ocean. *Nature*, 298,
489 2171-2173. doi:10.1126/science.1077445

490

491 Shen, H.T. (2003), Research on river ice processes: progress and missing links. *J. Cold Regions*
492 *Engineering*, 135-142.

493

494 Schirmermeister, L., Froese, D., Tumskey, V., Grosse, G., and Wetterich, S. (2013). "Yedoma: late
495 Pleistocene ice-rich syngenetic permafrost of Beringia," in *The Encyclopedia of Quaternary Science*,
496 ed. S. A. Elias (Amsterdam: Elsevier), 542–552. doi: 10.1016/b978-0-444-53643-3.00106-0

497

498 Shiklomanov, A.I., Lammers, R.B., (2009). Record Russian river discharge in 2007 and the limits of
499 analysis. *Environ. Res. Lett.* 112, 1–14. doi:10.1029/2006JG000352

500

501 Tananaev, N.I., (2016). Hydrological and sedimentary controls over fluvial thermal erosion, the Lena
502 River, central Yakutia. *Geomorphology* 253, 524–533. doi:10.1016/j.geomorph.2015.11.009

503

504 Tei, S., Morozumi, T., Nagai, S., Takano, S., Sugimoto, A., Shingubara, R., Fan, R., Fedorov, A.,
505 Gavrilyeva, T., Tananaev, N., Maximov, T., 2020. An extreme flood caused by a heavy snowfall over
506 the Indigirka River basin in Northeastern Siberia. *Hydrol. Process.* 34, 522–537.
507 doi:10.1002/hyp.13601
508
509 Walker, H.J. (1983). Erosion in a permafrost dominated delta, Proceedings Fourth International
510 Conference on Permafrost, Alaska. National Academy Press, Washington DC, 1344-1349.
511
512 Walker, H.J. and P. F. Hudson (2003), Hydrologic and Geomorphic Processes in the Colville Delta,
513 Alaska. *Geomorphology*, 56, 291-303. doi:10.1016/S0169-555X(03)00157-0
514
515 Yang D., D. Kane, L. Hinzman, X. Zhang, T. Zhang, and H. Ye (2002), Siberian Lena River hydrologic
516 regime and recent change. *J. of Geophys. Res.* , 107 (D23), 4694-4703. doi:10.1029/2002JD002542
517
518 Zhang, X., He, J., Zhang, J., Polyakov, I., Gerdes, R., Inoue, J., Wu, P. (2012). Enhanced poleward
519 moisture transport and amplified northern high-latitude wetting trend. *Nat. Clim. Chang.* 3, 47–51.
520 doi:10.1038/nclimate1631
521